COBEM 2021 26th International Congress of Mechanical Engineering
November 22-26, 2021, Virtual Congress, Brazil

COB-2021-1642
DYNAMIC STABILITY OF A CANTILEVERED VISCOELASTIC PIPE DISCHARGING INTERNAL FLUID

Lenin Lee Huaman Valdivia
Federal University of ABC
Lee.lenin@ufabc.edu.br

Juan Pablo Julca Avila
Federal University of ABC
Juan.avila@ufabc.edu.br

Abstract. *This work analyzes the dynamic stability of a cantilevered viscoelastic pipe discharging internal fluid. This is a non-conservative system because the internal flow supplies energy indefinitely to the pipe. The system loses stability by flutter when the flow velocity exceeds a critical value. When introducing the damping effect of viscoelastic material, a paradox arises: energy dissipation makes the system unstable. For energy dissipation, the Kelvin-Voigt viscoelastic model is used. The equation of motion is discretized by the Galerkin method. The critical velocity of the internal discharging fluid is obtained by analyzing the eigenvalues of the motion equation. The Argand stability diagram is presented for both elastic and viscoelastic pipes to carry out comparative studies. The effects of both the viscoelastic dissipation constant and the number of terms of the Galerkin series on the critical flow velocity, which depends on the mass parameter, are analyzed. Finally, the generalized coordinate response of the pipe is analyzed for two cases in the absence and presence of the viscoelastic dissipation parameter.*

Keywords: *Dynamic stability of pipes, Flow-induced vibration, Kelvin-Voigt model.*

1. INTRODUCTION

The extraction of gas and oil in deep-water has led to the development of FPSO (floating production storage and discharge) systems with pipes submerged in the sea for fluid extraction from the reservoirs. One of the challenges is comprehending the dynamic behavior of long pipes that hang freely from an FPSO that receives and injects fluids (oil, water, and gas). Moreover, these systems are subjected to extreme natural conditions such as ocean currents, high pressures, and temperature changes. The pipes hanging oscillate due to ocean currents, oscillations are not a problem if they are smooth and of small amplitudes. However, the velocity of the internal fluid in the pipe influences the oscillations, damping or amplifying in a harmful way that leads to a premature failure of the structure by fatigue.

This work analyzes the dynamic stability of a viscoelastic pipe discharging internal fluid, system is non-conservative, and the flow is viewed as an infinite source of energy for the system. This system has a paradigmatic behavior of instability by dissipation of energy intriguing in dynamics Païdoussis and Li (1993). Problems in pipe dynamics with fluid internal were studied in the 1950s by Ashley and Haviland (1950) in a theoretical attempt to explain the vibration observed in the Trans-Arabian Pipeline. Feodos'ev (1951), Housner (1952), and Niodson F.I. (1953) led the first study of the dynamics of pipes that contain fluid, simultaneously they obtained the correct linear equation to pipes supported at both ends. Bourrières (1939) first studied cantilevered pipes conveying fluid, obtained the general nonlinear equations of motion, and then linearized them. Benjamin (1961 a,b) studded on the dynamics of articulated cantilevers conveying fluid and established the Lagrange equations' appropriate form for this system.

In the early 1960s, research was carried out on loss of stability, when the flow velocity exceeds a critical value for cantilevered pipes containing internal fluid considering a viscoelastic dissipation constant. Theoretical research and experimental by Gregory and Païdoussis (1966a). Afterward, the second set of experimental tests was conducted by Greenwald & Dugundji (1967). Thomson and Tait (1879) showed that the instability of a general system is stabilized by gyroscopic force. Crandall (1995) showed that a stable system could turn unstable by introducing damping force. Semler et al. (1998) addressed the impact of damping factors in the stable dynamic for pipe containing internal fluid.

The structure of the article is: a brief introduction, mathematical model, results and discussions, and conclusions. In the results, it begins by reproducing the Argand diagram of a typical system, with the objective of introducing the reader to stability analysis. Subsequently, the effects of considering a viscoelastic dissipation factor are analyzed.

2. MATHEMATICAL MODEL

2.1 Equation of motion

The system consists of a cantilevered viscoelastic pipe, fixed at only end, discharging fluid as shown in "Figure 1". Pipe characteristics include a length L, mass per unit length m, flexural rigidity EI, dissipation viscoelastic constant E^*. The mass per unit length is M for fluid. The flow velocity is denoted by U. According to (Paidoussis, 2014), with the following considerations: (1) the system includes an inextensible slender pipe and of uniform section; (2) the lateral motions w to be small compared to the diameter; (3) the acceleration of axial fluid is zero with a fully-developed turbulent flow profile; (4) the pipe material is subjected to internal dissipation of the Kelvin-Voigt type; (5) the gravity, tensioning, and pressurization effect are neglected.

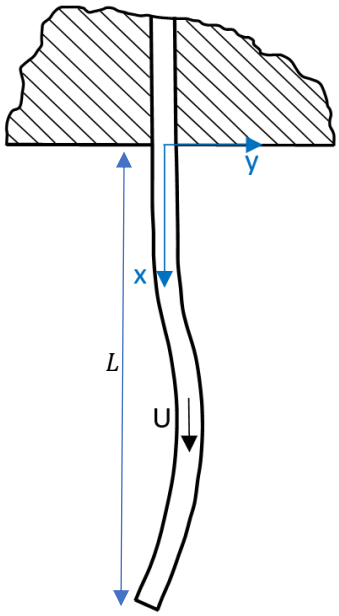

Figure 1. Cantilever viscoelastic pipe discharging internal fluid.

The linear equation of systems with small lateral motions (Paidoussis, 2014) is defined in Eq. (1):

$$\left(E^* \frac{\partial}{\partial t} + E\right) I \frac{\partial^4}{\partial x^4} + MU^2 \frac{\partial^2 w}{\partial x^2} + 2MU \frac{\partial^2 w}{\partial x \partial t} + (M+m) \frac{\partial^2 w}{\partial t^2} = p(t) \tag{1}$$

The axial and time coordinates are denoted by x and t, respectively. Lateral deflection is denoted as $w(x,t)$. The terms of Eq. (1) are identified as follows: the first term in the equation is the flexural restoring force (E is Young's modulus, E^* is Kelvin-Voigt dissipation constant, and I is area-moment of inertia), the second term is centrifugal force, the third term is associated with Coriolis force effect, the last term represents the inertial force of the fluid filled pipe. Being the excitation force $p(t)$.

The centrifugal force can destabilize the system when it is large enough to overcome the flexural restoring force. The Coriolis effect dampens the system as long as the flow velocity does not exceed the critical.

The Eq. (1) may be rendered dimensionless, the following non-dimensional quantities are defined:

$$\xi = \frac{x}{L}; y = \frac{w}{L}; u = UL\sqrt{\frac{M}{EI}}; \tau = t\sqrt{\frac{EI}{(M+m)L^4}}; \beta = \frac{M}{M+m}; \alpha = E^*\sqrt{\frac{I}{E(M+m)L^4}} \tag{2}$$

where u is the non-dimensional flow velocity, β is a mass parameter with a limit $0 < \beta < 1$, and α is the viscoelastic dissipation constant.

substituting Eq. (2) into Eq. (1) obtains the non-dimensional equation of motion as follows:

$$\frac{\partial^2 y}{\partial \tau^2} + 2\sqrt{\beta}u\frac{\partial^2 y}{\partial \tau \partial \xi} + \alpha\frac{\partial^5 y}{\partial \tau \partial \xi^4} + u^2\frac{\partial^2 y}{\partial \xi^2} + \frac{\partial^4 y}{\partial \xi^4} = p(\tau) \tag{3}$$

Following boundary conditions (displacement, slope, moment, or shear) for the cantilever pipe are:

$$\frac{\partial y}{\partial \xi}(0,\tau) = 0 \; ; \frac{\partial^3 y}{\partial \xi^3}(1,\tau) = 0 \; ; \frac{\partial^2 y}{\partial \xi^2}(1,\tau) = 0; \;\; y(0,\tau) = 0 \tag{4}$$

2.2 **Mode shapes of the cantilever pipe**

The model shapes of the cantilever pipe are obtained with four conditions Eq. (4), the simplest equation describing the flexural motion according to Euler-Bernoulli beam theory.

The frequency equation is:

$$cos(\lambda_r L) = -\left(\frac{1}{\cosh{(\lambda_r L)}}\right) \tag{5}$$

The model shapes or eigenfunctions, are:

$$\phi_r = A_1\left[\cos(\lambda_r \xi) - \cosh(\lambda_r \xi) - \frac{(\cos(\lambda_r L) + \cosh(\lambda_r L))}{(\sin(\lambda_r L) + \sinh(\lambda_r L))}(\sin(\lambda_r \xi) - \sinh(\lambda_r \xi))\right] \tag{6}$$

The transcendental equation Eq. (5) yields an infinite set of eigenvalues $\lambda_r L$. Substituting eigenvalues into Eq. (6), the mode shapes ϕ_r are obtained (Bishop and Johnson, 1960).

2.3 Discretization of the equation of motion

The non-dimensional equation of motion Eq. (3) can be discretized using the Galerkin method, let us consider the solution with the form:

$$y(\xi,\tau) = \sum_{r=1}^{N} \phi_r(\xi)\eta_r(\tau) \tag{7}$$

where $\phi_r(\xi)$ is the dimensionless model shapes of a cantilevered pipe, and $\eta_r(\tau)$ is the generalized coordinate of the discretized system. The force of excitation $p_r(\tau)$ in generalized coordinate is:

$$F_r(\xi,\tau) = \sum_{r=1}^{N} p_r(\tau)\eta_r(\tau) \tag{8}$$

The series in Eq. (7) and Eq. (9) may be truncated at a suitable value N. The generalized coordinates must be equal to the number of degrees N of freedom of system, it is clear that each set of equations represent a one-degree-of-freedom. For mode shapes, the orthogonality condition is given as:

$$\int_0^1 \phi_s(\xi)\phi_r(\xi)\, d\xi = \delta_{sr} \tag{9}$$

Substituting Eq. (7) into Eq. (3), the following expression is obtained:

$$\sum_{r=1}^{N} \phi'_r(x)\ddot{\eta}_r(\tau) + 2\sqrt{\beta}u\sum_{r=1}^{N} \phi'_r(x)\dot{\eta}_r(\tau) + \alpha\sum_{r=1}^{N} \phi''''_r(x)\dot{\eta}_r(\tau) + u^2\sum_{r=1}^{N} \phi''_r(x)\eta_r(\tau) + \sum_{r=1}^{N} \phi''''_r(x)\eta_r(\tau) = \sum_{r=1}^{N} p_r(\tau)\eta_r(\tau) \tag{10}$$

Substituting $\phi''''_r = \lambda_r{}^4 \phi_r$ and Eq. (9) into Eq. (10) and multiplying by $\phi_s(\xi)$, then integrating over zero to one, Eq. (11) is obtained:

$$\{\ddot{\eta}\} + \left[\alpha\lambda_r^4\delta_{sr} + 2\sqrt{\beta}uB_{sr}\right]\{\dot{\eta}\} + [\lambda_r^4\delta_{sr} + u^2C_{sr}]\{\eta\} = \{F\} \tag{11}$$

Where δ_{sr} is Kronecker's delta, B_{sr} end C_{sr} are matrix of order $n \times n$; α, β, λ and u are non-dimensional parameters.

B_{sr} and C_{sr} are defined as follows:

$$B_{sr} = \int_0^1 \phi_s(x)\, \phi_r' d\xi \tag{12}$$

$$C_{sr} = \int_0^1 \phi_s(x)\, \phi_r'' d\xi \tag{13}$$

Another method to obtain C_{sr} and B_{sr}, is considering the properties of eigenfunction, given by:

$$B_{sr} = \frac{4}{(\lambda_s/\lambda_r)^2 + (-1)^{r+s}} \; ; \quad C_{sr} = \frac{4(\lambda_r\sigma_r - \lambda_s\sigma_s)}{(-1)^{r+s} - (\lambda_s/\lambda_r)^2} \quad \text{for } s \neq r \tag{14}$$

$$B_{sr} = 2 \qquad ; \quad C_{sr} = \lambda_r\sigma_r(2 - \lambda_r\sigma_r) \quad \text{for } s = r \tag{15}$$

the vectors $\{\eta\}$ and $\{F\}$ are defined as:

$$\{\eta\} = \begin{Bmatrix} \eta_1(\tau) \\ \vdots \\ \eta_n(\tau) \end{Bmatrix}; \{F\} = \begin{Bmatrix} F_1(\tau) \\ \vdots \\ F_n(\tau) \end{Bmatrix} \tag{16}$$

The element F_r is defined as:

$$F_r = \int_0^1 p(\tau)\, \phi_r(\xi) d\xi \tag{17}$$

The motion equation of the system given at Eq. (11) can be represented in a matrix formulation as follows:

$$[M]\{\ddot{\eta}\} + [C]\{\dot{\eta}\} + [K]\{\eta\} = \{F\} \tag{18}$$

Where $[M]$, $[C]$, and $[K]$ are the mass, dissipation, and stiffness matrices of order nxn, respectively; $\{\eta\}$ is the vector of generalized coordinates, and $\{F\}$ is input force vectors.

$$[M] = \delta_{sr} \tag{19}$$

$$[C] = \alpha\lambda_r^4\delta_{sr} + 2\sqrt{\beta}uB_{sr} \tag{20}$$

$$[k] = \lambda_r^4\delta_{sr} + u^2C_{sr} \tag{21}$$

2.4 Analysis of frequencies

The frequency analysis is necessary to predict the onset of the system instability by flutter. In general, the system will be stable or unstable according to frequency ω; if the imaginary component $Im(\omega)$ is positive or negative, the system is stable or unstable, respectability.

The motion equation Eq. (11) is discretized to calculate the frequencies in the absence of exciting force $\{F\}$, considering the solution of Eq. (11) may be expressed as:

$$\eta(\tau) = \sum_{r=1}^{N} a_r e^{i\omega t} \tag{22}$$

Substituting the assumed solution of Eq. (22) into Eq.(11), gives:

$$\sum_{r=1}^{N}\left[(\lambda_r^4 - w^2 + \alpha\lambda_r^4 i\omega)\delta_{sr} + u^2 C_{sr} + 2\sqrt{\beta}uB_{sr}\right]a_r e^{i\omega t} = 0, s = 1,2,3 \dots N \tag{23}$$

The frequencies are obtained using the non-trivial solution of Eq. (23).

$$\det\left(\sum_{r=1}^{N}\left[(\lambda_r^4 - w^2 + \alpha\lambda_r^4 i\omega)\delta_{sr} + u^2 C_{sr} + 2\sqrt{\beta}uB_{sr}\right]\right) = 0, s = 1,2,3 \dots N \tag{24}$$

The solutions obtained by solving Eq. (24) are of infinite order. Nevertheless, they can be adequately reduced to solutions of order N.

2.5 Dynamic response

The method of Laplace transform ($\mathcal{L}$) is taking of Eq. (11), considering the following initial conditions $\eta(0) = \dot{\eta}(0) = \ddot{\eta} = 0$, the following expression is obtained:

$$(s^2[M] + s[C] + [K])\mathcal{L}(\{\eta(\tau)\}) = \mathcal{L}(\{F\}) \tag{25}$$

defining the following matrix:

$$[H] = (s^2[M] + s[C] + [K])^{-1} \tag{26}$$

multiplying Eq. (25) by Eq. (26) and taking the inverse Laplace transformation ($\mathcal{L}^{-1}$), the following expression is obtained:

$$\{\eta(\tau)\} = \mathcal{L}^{-1}([H]\mathcal{L}(\{F\})) \tag{27}$$

The response of the generalized coordinate $\eta(\tau)$ is calculated using Eq. (27).

3. RESULTS AND DISCUSSION

3.1 The Argand diagram -the frequency as a function of discharge flow velocity

Independent motion parameters define the system:α, β, and u are the viscoelastic dissipation constant, mass parameter, and flow velocity, respectively. The frequencies are calculated by increasing the values of non-dimensional flow velocity u, starting from $u = 0$ to $u = 14$, with intervals of $\Delta u = 0.05$.

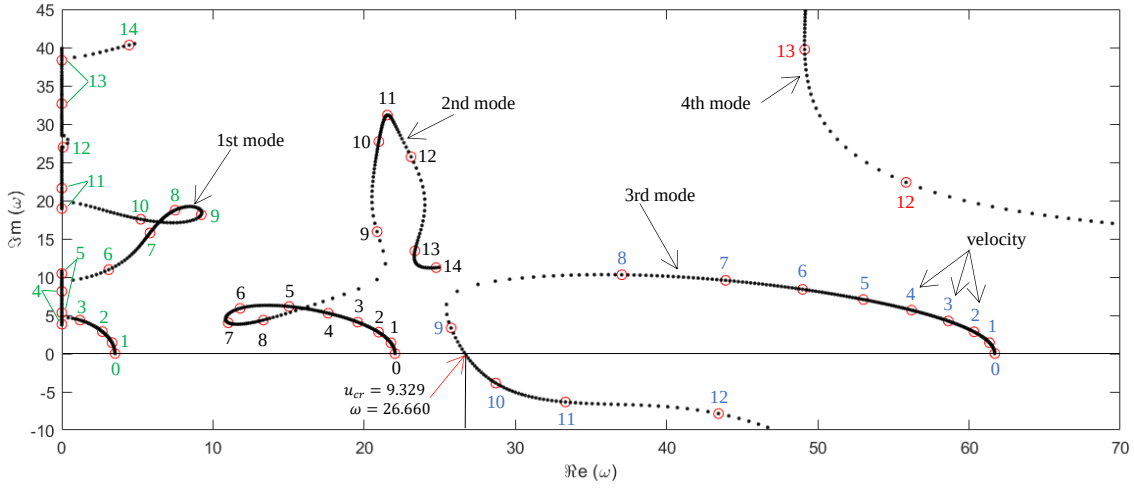

Figure 2. The Argand diagram obtained with N=6, $\beta = 0.5$, $\alpha = 0$ (Sazesh and Shams, 2019).

The beginning of instability by the Hopf bifurcation occurs when for one mode the diagram crosses the instability axis, the real component of the frequency is zero ($Re(\omega) = 0$), and flow velocity matches critical flow velocity ($u = u_{cr}$). The system loses stability by flutter for flow velocities greater than the critical flow velocity ($u > u_{cr}$).

"Figure 2" shows the frequency in the Argand diagram with increasing flow velocity for the first four modes, considering a system in absent dissipation effect of material ($\alpha = 0$). The flow-induced damping in all system modes for velocity flow $u < 3$, approximately. The system stable and dampened for flow velocity $u < 9.329$. The Hopf bifurcation occurs at $u = u_{cr} = 9.329$ in the third mode with $\omega_{cr} = 26.660$, and the system becomes unstable by flutter. For flow velocity within ranges $9.329 < u < 14$, the system is unstable. The instability by flutter is not always due to the third mode. The mode that causes flutter and critical flow velocity depends on the value of β.

The buckling instability does not occur, none of the modes cross from positive to negative axis on the imaginary axis itself.

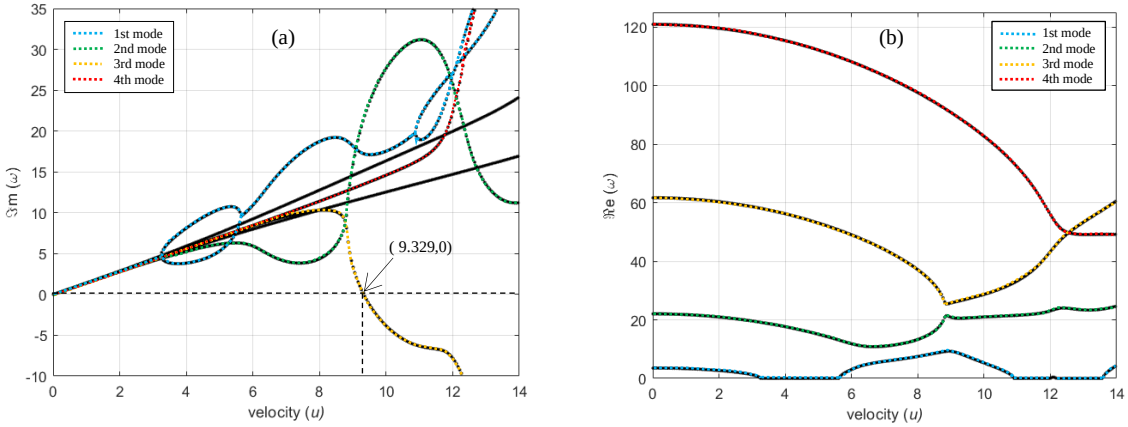

Figure 3. The real and imaginary components of the dimensionless complex as functions of the dimensionless flow velocity, (a) imaginary component of frequency for *N*=6; (b) real component of frequency for *N*=6.

The Argand diagram, or stability, "Figure 2" does not adequately show the behavior of the modes when this is on the imaginary axis. When one mode hits the imaginary axis, it branches, and when leaving the imaginary axis, it joins, so it is better to analyze frequency components separately versus the flow velocity.

"Figure 3 (a)" shows the imaginary component of the frequency as a function of flow velocity, $Im(\omega)$ is associated with of damping of the system, when the imaginary component is positive ($Im(\omega)$>0), the flow velocity less than critical velocity ($u < u_{cr}$). The imaginary component of the frequency of the third mode crosses from the positive to the negative plane ($Im(\omega)$=0) in $u_{cr} = 9.329$, the system becomes unstable.

"Figure 3 (b)" shows that at early stages ($u < 3$), the increase of flow velocity has stabilizing effects on the system, Re (ω) decreases as the velocity flow increases, the oscillation frequency of the system decreases.

Table 1. Critical velocity is obtained when the cantilever pipe is discharging internal fluid.

	Greenwald Dundji's 1967	**Ni et al., 2011**	**Obtained values**	**Type of instability**	**Instability from**
Critical velocity	9.32	9.328	9.329	flutter	3rd mode

(1) $N = 6$, $\beta = 0.5$, and $\alpha = 0$

"Table 1" compares the obtained critical flow velocity with the results found in the literature, a very well agreement was shown results similar. Experimental value obtained by Greenwald Dundji's (1967) and theorical value obtained by Ni et al., (2011) using method of the differential quadrature method (DQM).

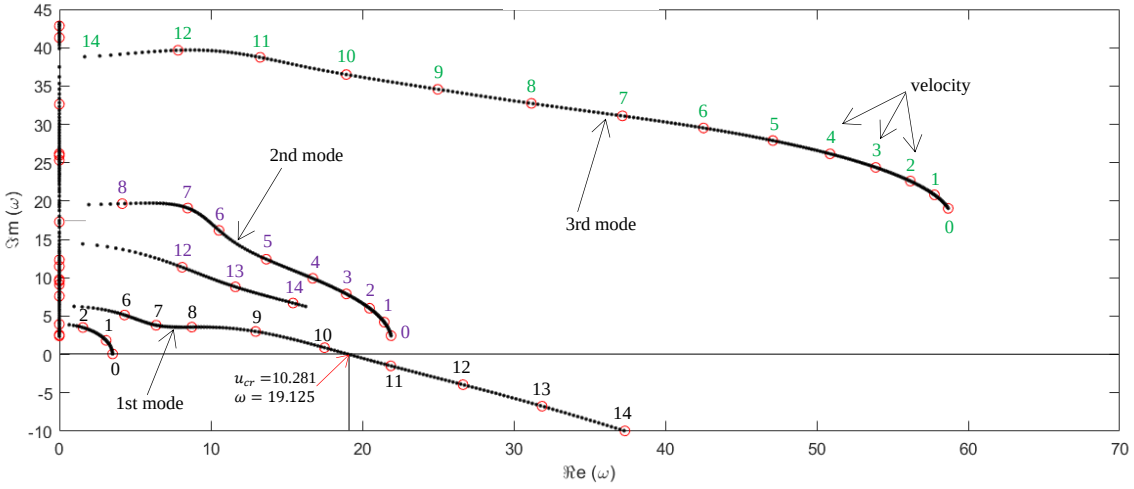

Figure 4. The Argand diagram obtained with $N = 6$ terms, $\beta = 0.8$, $\alpha = 0.01$

"Figure 4" shows the frequency in the Argand diagram with increasing flow velocity, for the first three modes, the system considering dissipation effect of material ($\alpha = 0.01$). The flow-induced damping in all system modes for velocity flow $u < 2$, approximately. The system is dampened for flow velocity $u < 10.281$. The Hopf bifurcation occurs at $u = u_{cr} = 10.28$ in the first mode with $\omega_{cr} = 19.125$, and the system becomes unstable by flutter. For flow velocity within range $10.281 < u < 14$ the system is unstable.

Table 2. Critical flow velocity obtained for a cantilever viscoelastic pipe discharging internal fluid.

	Value u_{cr}	**Frequency ω_{cr}**	**Type of instability**	**Instability from**
Critical velocity	10.281	19.125	Flutter	1st mode

(1) N=6, $\beta = 0.8$, and $\alpha = 0.01$

"Table 2" summarizes critical flow velocity and type of instability obtained by analyzing "Figure 4".

3.2 Critical discharge flow velocity

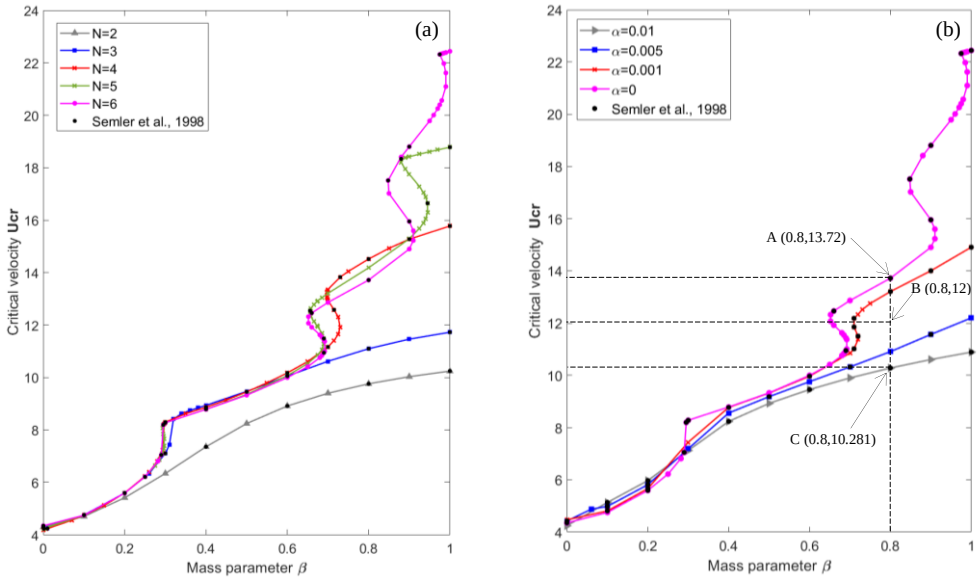

"Figure 5" (a) critical flow velocity versus β, increasing the model shapes (N) considering no damping ($\alpha = 0$); (b) critical flow velocity versus β, increasing the viscoelastic dissipative constant and considering six model shapes (N=6).

"Figure *5* (a)" presents the stability curve obtained for a different number of terms. It is important to note that for: *N*=2, a smooth curve is obtained; for *N*=4, there is the first jump around $\beta = 0.3$ and a second jump around $\beta = 0.7$; and for *N*=6, numerous jumps are observed around $\beta = 0.3, 0.65, 0.9,$ and 0.95. The jump increase is associated with a new generalized coordinate.

"Figure *5* (b)" shows considering *N*=6 the curves of critical velocity for different viscoelastic dissipation constants of the material. Viscoelastic dissipation constant $\alpha = 0.01$ corresponds to elastomer pipes, and the value of $\alpha = 10^{-3}$ or less corresponds to metal (Snowdon, 1968). The viscoelastic effect of the material is analyzed in ranges: In the first range, $\beta < 0.3$, an increase in the viscoelastic dissipation constant generates a stabilizing effect in the system; In the second range, $\beta > 0.3$, the increase of the viscoelastic dissipation constant has a destabilizing effect. Therefore, for large value of viscoelastic dissipation constant, does not follow usual patron to stabilize the system by dissipation energy paradoxically. Increasing of the value of the viscoelastic dissipation constant (α) has an opposite effect to the generalized coordinate increment. The increase in the viscoelastic dissipative constant kills the jumps generated by the increase of the generalized coordinates.

"Figure *5* (b)" show that for $\beta = 0.8$ without considering a viscoelastic dissipative constant of the material ($\alpha = 0$), the critical flow velocity is $u_{cr} = 13.72$. However, if a viscoelastic dissipative constant ($\alpha = 0.01$) is considered, the new critical flow velocity is $u_{cr} = 10.281$.

3.3 Response in generalized coordinates of the system

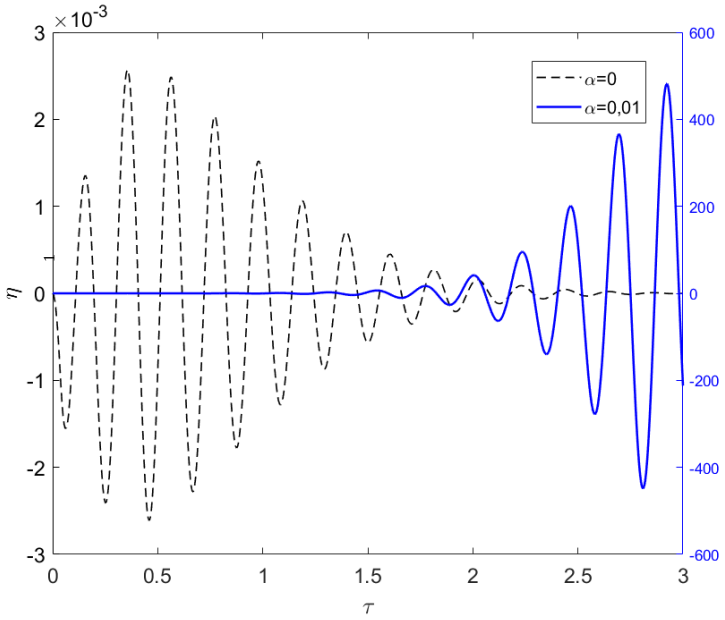

Figure 6. Response of the generalized coordinate $\eta_1(\tau)$, considering: $\beta = 0.8$, $u = 11$ and $p_r = sin\ (\tau)$

"Figure 6" compares the response in generalized coordinates for two systems, both with the same internal flow velocity $u = 12$. The dashed line represents how the response dampens over time (system stable) for an elastic tube $\alpha = 0$; while the solid line shows the response for a viscoelastic tube with viscoelastic dissipation constant $\alpha = 0.01$, in contrast, the amplitudes of the oscillations of response are amplified in time (system unstable).

Considering a viscoelastic tube implies a viscoelastic dissipative constant in the equation of motion Eq. ((1), this constant impacts the critical flow velocity and reduces the range of velocities in which the system is stable.

"Figure *5* (b)" shows the results for a system with $\beta = 0.8$ and $u = 12$. For these conditions, the system is represented at point B, and the stability is analyzed as follows:

(a) For a purely elastic pipe ($\alpha = 0$): the critical flow velocity is at point A ($u_{cr} = 13.72$), the velocity of the fluid is less than the critical flow velocity; therefore, the system is stable ($u_{cr} > 12$).

(b) For a viscoelastic tube ($\alpha = 0.01$): the critical flow velocity is at point C ($u_{cr} = 10.281$), the flow velocity is greater than the critical flow velocity; therefore, the system is unstable ($u_{cr} < 12$).

4. CONCLUSION

For systems with flow velocity less than the critical flow velocity ($u < u_{cr}$), the obtained frequencies are positive, the system loses energy, and the oscillations are dampened. Conversely, when the flow velocity is greater than the critical flow velocity ($u < u_{cr}$), the system gains energy and amplifies the oscillation.

The damping effect of the viscoelastic material of the Kelvin-Voigt is slightly positive for $\beta < 0.3$, and it presents additional damping caused by Coriolis forces. For $\beta > 0.3$, the effect is negative, decreasing the velocity range in which the system is stable.

The cantilever viscoelastic pipe can be destabilized by dissipation, and it is associated with flutter in the first mode for a system with $\beta = 0.8$, $\alpha = 0.01$ e $u = 12$.

5. REFERENCES

Ashley and Haviland, 1950. Holt Ashley and George Haviland. Bending Vibrations of a Pipe Line Containing Flowing Fluid. *Journal of Applied Mechanics*. 17, 3 (Sep.-1950), 229–232. doi: 10.1115/1.4010122.

Benjamin, T.B., A 1961a. T. B. Benjamin and Proc R. Soc Lond A. Dynamics of a system of articulated pipes conveying fluid - I.Theory. *Proceedings of the Royal Society of London. Series A. Mathematical and Physical Sciences*. 261, 1307 (1961), 457–486. doi: 10.1098/rspa.1961.0090.

Benjamin, T.B., 1961b. Dynamics of a system of articulated pipes conveying fluid. II. Experiments. Proceedings of the Royal Society (London) A 261, 487-499.

Bishop, R.E.D. and Johnson D.C 1960, 1979 *The Mechanics of Vibration*. Cambridge: Cambridge University Press.

Stephen H. Crandall, 1995. The effect of damping on the stability of gyroscopic pendulums. *Theoretical, Experimental, and Numerical Contributions to the Mechanics of Fluids and Solids*. (1995), 761–780. doi: 10.1007/978-3-0348-9229-2_39.

Greenwald, A.S. and Dugundji, J., 1967. Static and dynamic instabilities of a propellant line. MIT Aeroelastic and Structures Research Lab, AFOSR Sci. Report: AFOSR 67-1395.

Gregory, R.W. and Païdoussis M.P., 1966a Unstable oscillation of tubular cantilevers conveying fluid. I. Theory. *Proceedings of the Royal Society (London)* A 293, 512-527.

Gregory, R.W. and Païdoussis M.P., 1966b Unstable oscillation of tubular cantilevers conveying fluid. II. Experiments. *Proceedings of the Royal Society (London)* A 293, 528-542.

Housner, 1952. Bending Vibrations of a Pipe Line Containing Flowing Fluid. *Journal of Applied Mechanics*. 19, 2 (1952), 205–208. doi: 10.1115/1.4010447.

Ni, Q., Zhang, Z.L. and Wang, L., 2011. Application of the differential transformationmethod to vibration analysis of pipes conveying fluid. *Applied Mathematics and Computation* 217, 7028-7038.

Niordson, F.I., 1953. Vibrations of a cylindrical tube containing flowing fluid. *Kungliga Tekniska Hogskolans Handlingar (Stockholm)* No. 73.

Païdoussis M.P., 2014. *Fluid-structure interactions. Volume 1, Slender structures and axial flow*.

Païdoussis and Li, 1993. M. P. PaÏdoussis and G. X. Li. Pipes conveying fluid: A model dynamical problem. *Journal of Fluids and Structures*. doi: 10.1006/jfls.1993.1011.

Sazesh and Shams, 2019. Saeid Sazesh and Shahrokh Shams. Vibration analysis of cantilever pipe conveying fluid under distributed random excitation. *Journal of Fluids and Structures*. 87, (2019), 84–101. doi: 10.1016/j.jfluidstructs.2019.03.018.

Semler, C., Alighanbari H. and Païdoussis M.P., 1998. A physical explanation of the destabilizing effect of damping. *Journal of Applied Mechanics* 65, 642-648.

Snowdon J.C., *1968. Vibration and Shock in Damped Mechanical Systems. New York: John Wiley.*

Thomson, W and Tait, G., 1879 *A Treatise on Natural Philosophy*, Vol. 1, Part I, p. 370. Cambridge: Cambridge University Press.